

Pure Pursuit Control Method Based on SVR Inverse-model for Tractor Navigation

Zhang Wenyu Ding Youchun Wang Xueling Zhang Xing Cai Xiang Liao Qingxi
(College of Engineering, Huazhong Agricultural University, Wuhan 430070, China)

Abstract: Considering fact that uncertain longitudinal slip of tire and uncertain pavement leads to problem that trajectory of tractor could not be accurately described by kinematic model, a pure pursuit Controlling method based on SVR inverse-model was proposed for agricultural machine navigation. This paper analyzed and determined main structure and technical parameters of method. The inverse-model for forward heading of tractor was established by using method of granular support vector regression, and the corresponding relation function of kinematic theoretical curvature and actual curvature was obtained. The error of pure pursuit navigation model was corrected via inverse-model, thus the adaptability and dynamic performance of pure pursuit Controlling method were improved. The path tracking experiments of navigation system for tractor was conducted, which showed that the maximum of linear tracing pitch yaw roll error was less than 0.061 4 m when the speed of agricultural machinery was 1.2 m/s and path length was longer than 125 m. Compared with the method of conventional pure pursuit navigation model, the pure pursuit Controlling method based on SVR inverse-model has better linear tracking performance. Field experiment results indicated that the maximum lateral deviation was 0.088 7 m when the running speed of the tractor was 0.5m/s. Meanwhile, the controller significantly improved precision of field experiment. Based on path tracking experiments and field experiments, the navigation Controlling method could be applied to automatic row-controlled operation of 2BFQ-6 type direct-seeding combined dual purpose planter for rapeseed.

Key words: tractor; navigation; inverse-model; support vector regression; pure pursuit model

0 Introduction

Controlling method of farm path tracking was key technique of intelligent navigation^[1-2]. It was studied by many scholars at home and abroad including proportion integration differentiation control^[3-4], fuzzy control^[5-6], optimal control^[7-8] and pure pursuit control^[9-10]. Proportion integration differentiation control and fuzzy control didn't rely on specific mathematical models. However, optimal control and pure pursuit control relied on specific mathematical models. Fuzzy control, genetic algorithm and particle swarm optimization controller were used to optimize parameters by Li et al^[9], Zou et al^[11] and Meng et al^[12], respectively. Therefore, nevertheless few mathematical models were optimized. Kinematic model

was optimized by Erkan et al^[13] who used stimulus-response method identification method. However, Linear model had limit fitting capability. Self-tuning controller was used to optimize kinematic model by Bai et al^[14], which could improve tracking performance of curve path and could not improve tracking performance of line path. Neural networks were used to turn identification system model by Zhu et al^[15] and Hamzaoui et al^[16]. The neural networks had high robustness and nonlinear fitting capabilities, however it required many training samples, and real-time computing performance was weak and easy to fall into local minimum solution. Appropriate modeling approach could improve control quality.

In order to establish high-precision navigation tractor models for improving tractor linear tracking accuracy,

Received date: 2015-07-09 Accepted date: 2015-08-09

Supported by Special Fund for Technical System of National Rape Industry (Grant No. CARS-13), Special Fund for Agro-scientific Research in Public Interest(Grant No. 201503116-6), Fundamental Research Funds for Central Universities(Grant Nos. 2013PY033, 2014PY033), and Wuhan High and New Technology Industry Scientific and Technological Innovation Team (Grant No. 2014070504020240)

Author: Zhang Wenyu, Doctor of philosophy. E-mail: zhangwy@webmail.hzau.edu.cn. Tel: +86-15072344412.

Corresponding author: Liao Qingxi, Professor. E-mail: liaoxq@mail.hzau.edu.cn. Tel: +86-13871094327.

SVR (Support vector regression) model based on tractor navigation inverse model of pure pursuit controlling method was proposed. SVR regression method was based on structural risk minimization. It is more stable and stronger generalization ability than conventional methods, because it used small samples and statistical learning methods to establish regression model. Navigation controller was designed by using this method. The controller could be applied to automatic row-controlled operation of 2BFQ-6 type direct-seeding combined dual purpose planter for rapeseed.

1 Structure of tractor navigation system

With navigation objects as Dongfanghong-LX854 tractor for 2BFQ-6 type direct-seeding combined dual purpose planter for rapeseed. The system was divided into hardware and software. The hardware included RTK-GNSS systems, DWQT-BZ-V-60-G-type angle sensor, NI-USB-6216 data card, TPC6000-6100T type IPC and steering actuators. The software was pure pursuit inverse model control based on SVR. SINAN M300 RTK-GNSS system was used to receive location information. DWQT-BZ-V-60-G-type angle sensor and NI-USB-6216 data card was used to collect signal of front wheel angle. Navigation controller operation output steering control signal that was based on pose information and angle signal. Full hydraulic steering control valve system made tractor to navigate by signal of pure pursuit control inverse-model control. The system is presented in Fig. 1.

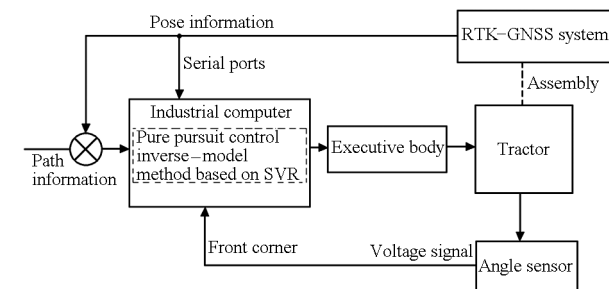


Fig. 1 Structure diagram of navigation system

2 Design of pure pursuit control method based on SVR inverse-model

Four parts of pure pursuit control method based on SVR inverse-model were Kalman filter, pure pursuit model, SVR inverse-model and variable universe fuzzy

controller^[18]. The structure of pure pursuit control method based on SVR inverse-model was visualized in Fig. 2.

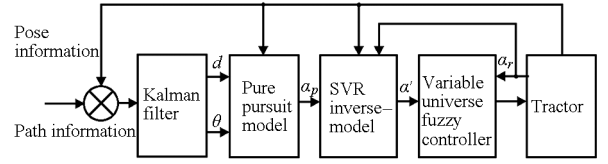


Fig. 2 Schematic block of pure pursuit control method based on SVR inverse-model

where θ is deviation of heading angle with angle of path direction; α_p is the turning angle from pure pursuit model; α' is turning angle from SVR inverse-model; α_r is the realized steering angle.

2.1 Design of Kalman filter

Error of SINAN M300 type RTK-GNSS system was ± 1.5 cm. Meanwhile, there were other errors that caused by tilt and shake of tractor. Sampling error also could not be ignored. They will affect quality of controller navigation path. For improving location accuracy, the Kalman filter algorithm was introduced to process the initial locating results^[19]. By using Kalman filter, this algorithm could filter handle deviations of lateral and direction. According to data of preliminary test, Q_d was processed incentive noise covariance-driven of lateral deviation d , it was set to 0.1. R_d was measured noise covariance-driven of lateral deviation, and it was also set to 0.1. Q_θ was processed incentive noise covariance-driven of direction deviation θ , it was set to 0.6. R_θ was measured noise covariance-driven of direction deviation, it was also set to 0.8. Combining Kalman filter prediction and linear interpolation, position of tractor could make up in sampling interval. Experiments showed that this algorithm could effectively improve speed adaptability.

2.2 Design of pure pursuit controller

2.2.1 Kinematics model of the tractor

The simple kinematics model for tractor was established, because some factors were difficult to measure including longitudinal slip of tire and axle rigidity. The kinematic model of tractor was similar to the well-known bicycle model^[15]. The kinematic model of tractor was given as follow

$$\theta' = \frac{v \tan \alpha}{l} = \gamma v \quad (1)$$

where θ' was change rate of the heading angle; α was

the front wheel turning angle; v was the real-time speed; l was the wheelbase and γ was turning curvature.

2.2.2 Design and improvement of pure pursuit model

Pure pursuit model was used for calculating path of tractor by choosing suitable beforehand point^[10] as Fig. 3. Where L_d was distance of beforehand point, R was turning radius of tractor and O was center of a circle.

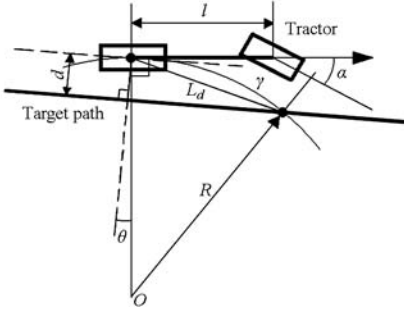


Fig. 3 Geometric diagram of pure pursuit model

Function in accordance with the geometry of pure pursuit model shown in Fig. 3.

$$\gamma = \frac{2(d \cos \theta - \sqrt{L_d^2 - d^2} \sin \theta)}{L_d^2} \quad (2)$$

Eqs. (1) and (2) could be integrated to obtain α .

$$\alpha = \arctan \frac{2l(d \cos \theta - \sqrt{L_d^2 - d^2} \sin \theta)}{L_d^2} \quad (3)$$

When the value of L_d was determined, d and θ were determinants of front wheel turning angle α . There was only one controllable parameter L_d . The system could not adjust the control strategy flexibly when forward speed of tractor is different. Therefore, it introduced two adjustment coefficients ξ_1 and ξ_2 . ξ_1 affected control effectiveness of d in the modified model, and ξ_2 affected control effectiveness of θ . ξ_1 and ξ_2 respectively affected control accuracy and stability of tracking system.

$$\alpha = \arctan \frac{2l(\xi_1 d \cos \theta - \xi_2 \sqrt{L_d^2 - d^2} \sin \theta)}{L_d^2} \quad (4)$$

L_d , ξ_1 and ξ_2 varied with speed v of tractor change. The system stability was more important when the speed v was high. Therefore, it would reduce ξ_1 , increase ξ_2 and L_d in the high speed. The method improved system stability under premise of ensuring accuracy. The relation was as follows

$$\begin{cases} L_d = \begin{cases} 1.6 + \min(1.5(v - 0.7), 1.6) & (v > 0.7) \\ 1.6 & (v \leq 0.7) \end{cases} \\ \xi_1 = \begin{cases} 1 & (v > 0.7) \\ 1 + 0.6(0.7 - v) & (v \leq 0.7) \end{cases} \\ \xi_2 = \begin{cases} 1 + \min(0.5(v - 0.7), 1.2) & (v > 0.7) \\ 1 & (v \leq 0.7) \end{cases} \end{cases} \quad (5)$$

According to Eqs. (4) and (5), the pure pursuit controller was designed.

2.3 Design of inverse-model based on SVR

The accuracy of control model was improved by establishing inverse-model. Because there were effected longitudinal slip of tire, pavement properties, vehicle angle and sensor system error. Kinematic model could not accurately describe trajectory of tractor. Meanwhile, it was difficult to deduce model from forward direction. The data of θ' and α_r were recorded to design inverse-model of relationship between θ' and α_r . The inverse-model was used to correct control error that caused by simplification kinematics model. The errors of θ' data were so larger that it is impossible to establish model, therefore, the original θ' data was processed by Gauss-granular pretreatment. Structure of inverse-model by granular support vector regression was shown in Fig. 4. Where $\{\alpha_r, \alpha'_m\}$ was the set of Gauss-granular.

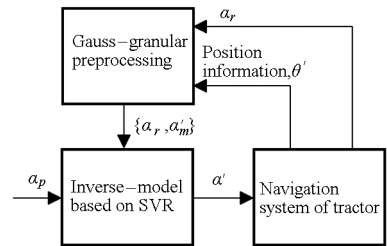


Fig. 4 Structure of inverse-model by granular support vector regression

2.3.1 Gauss-granular pretreatment

In order to establish relationship between actual turning curvature γ_r and theoretical curve curvature γ_m , it was introduced theoretical front wheel turning angle α_m . γ_r and α_r were recorded by navigation system that was based on Eq. (1), the γ_m and α_m were calculated in Eq. (6).

$$\begin{cases} \alpha_m = \arctan(\gamma_r l) = \arctan\left(\frac{\theta'}{v} l\right) \\ \gamma_m = \frac{\tan \alpha_r}{l} \end{cases} \quad (6)$$

Eq. (6) showed that relationship of actual turning

curvature γ_r and theoretical curve curvature γ_m could be transformed into relationship of α_m and α_r . It was $\alpha_m = f(\alpha_r)$. α_p was calculated by pure pursuit model, then used to get correction turning angle α' by relationship model of α_m with α_r . α_p corresponded to theoretical front wheel turning angle of pure pursuit model. α' was actual need turning angle for achieving theoretical curve curvature.

θ' and v were used to obtain α_m by Eq. (6), θ' was calculated from position information. Sampling frequency of position of RTK - GNSS was 2 Hz, therefore, frequency of α_m data was also 2 Hz. Sampling frequency of NI - USB - 6216 data card was 5 000 Hz, α_r was average value of 500 data, and frequency of α_r was 10 Hz. In order to make α_r and α_m to have same frequency, the average value of A in the location signal scan interval was used to set up the data set $A: \{\alpha_r, \alpha_m\}$.

α_r and α_m data corresponded to the distribution map as shown in Fig. 5. Error of measurement was caused by error of system. The efficiency and accuracy of model that use the original data were low and difficult to improve control accuracy.

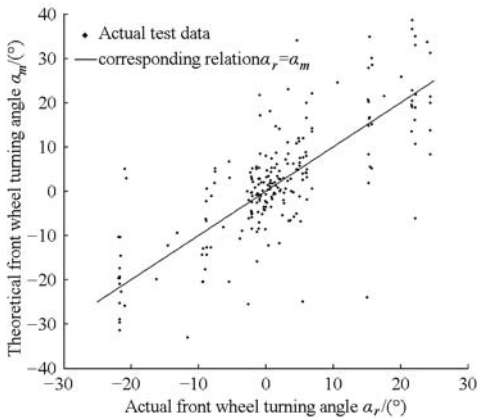


Fig. 5 Relation graph of theory and practice front wheel angle

It was difficult to obtain a precise mathematical model. Therefore, data should pre-process by Gauss-granular method. The method was to replace data of a certain range with a certain rule to a granular. Because α_r was measured with high accuracy. The data were preprocessed by longitudinal granularity method. The method steps were showed as follows:

(1) Within a certain range which center was α_{ri} and width was 2μ (α_r, α_m) data was constructed into a granularity. Granularity size of information granularity was $[\alpha_{ri} - \mu, \alpha_{ri} + \mu]$.

(2) In the range α_m data was averaged by Gauss

weighted, the center point of range was α_{ri} .

$$\begin{cases} w_j = e^{-(\alpha_r - \alpha_{ri}) / (2\sigma^2)} \\ \alpha'_{mi} = \frac{\sum_{j=1}^n w_j \alpha_{mj}}{\sum_{j=1}^n w_j} \end{cases} \quad (7)$$

where j was sequence number of data in the range of information granularity; n was sample size of information granularity; w_j was Gauss weighted; σ was the standard deviation of Gauss function, and α'_{mi} was values of information granularity.

(3) Values of α'_{mi} was calculated form a set ($\alpha_{ri}, \alpha'_{mi}$) of granularity.

Width of set was determined by width of front wheel turning angle α_r . α_r was varied greatly ($\pm 10^\circ$) when Tractor was turning or adjusted. α_r was varied smaller when tractor was steady tracking state, its range reaches $\pm 2^\circ$. The adaptability of method that used to fix width 2μ was low. Therefore, the dynamic granularity method was used to solve the problem of particle size adaptability. The width 2μ of information granularity changes with overall width of set A . The dynamic granularity calculation steps of data set were showed as follows:

(1) According to the width $\alpha_r \in [\alpha_{rmin}, \alpha_{rmax}]$ of original data set A , width 2μ of the information granularity was determined.

$$\mu = (\alpha_{rmax} - \alpha_{rmin}) / n' \quad (n' = 24)$$

(2) Granularity center was α_{ri} .

$$\alpha_{ri} = \alpha_{rmin} + i\mu \quad (i = 1, 2, \dots, n')$$

(3) Structuring information granularity was based on α_{ri} and μ . And the adjacent information granularity range was partially overlap, which enhances the granularity data linearity. σ was set to $\mu/2$, α'_{mi} was calculated according to the granularity method above. new set $\{\alpha_r, \alpha'_{mi}\}$ of dynamic granularity data was composed.

2.3.2 Application of support vector regression

SVR support vector regression method was used to identify and build model from set $\{\alpha_r, \alpha'_{mi}\}$. Fitting the data is $\{(x_i, y_i), i = 1, 2, \dots, l\}$, $x_i \in \mathbf{R}_n$, l was sample size. In this paper, $x = \alpha_r$ and $y = \alpha'_{mi}$. SVR was realized through practical problems were mapped to high-dimensional feature space by nonlinear mapping, structure linear discriminant function in high dimensional space realized non-linear regression

function of original space.

$$f(x) = \mathbf{w}^T \boldsymbol{\varphi}(x) + b$$

where \mathbf{w} was the weight vector, $\boldsymbol{\varphi}(x)$ is nonlinear onlinear mapping of high-dimensional feature space, b was a bias term.

In order to improve the robustness of method, this method introduced insensitive loss factor ε , loss function was L (in Eq. (8)). The definition of value is loss less when the error of model with the actual value was less than ε .

$$L(y, f(x), \varepsilon) = \begin{cases} 0 & (|y - f(x)| \leq \varepsilon) \\ |y - f(x)| - \varepsilon & (|y - f(x)| > \varepsilon) \end{cases} \quad (8)$$

Minimizing risk of high-dimensional feature space function was based on the SRM principle. Therefore, the problem was equivalent to $\|\mathbf{w}\|^2$ minimization problem. The complexity of fitting function was reduced by relaxation factor ζ_i and the penalty factor C . the function was showed as follow

$$\begin{cases} \min_{\mathbf{w}, b, \zeta, \zeta^*} \frac{1}{2} \mathbf{w}^T \mathbf{w} + C \sum_{i=1}^l \zeta_i + C \sum_{i=1}^l \zeta_i^* \\ \text{s. t. } \mathbf{w}^T \boldsymbol{\varphi}(x_i) + b - y_i \leq \varepsilon + \zeta_i \\ y_i - \mathbf{w}^T \boldsymbol{\varphi}(x_i) - b \leq \varepsilon + \zeta_i^* \\ (\zeta_i \geq 0, \zeta_i^* \geq 0, i = 1, 2, \dots, l) \end{cases} \quad (9)$$

The Lagrange function was introduced to solve the minimization problem. The problem was further transformed into a dual problem

$$\begin{cases} \min_{\beta, \beta^*} \frac{1}{2} (\beta - \beta^*)^T Q (\beta - \beta^*) + \\ \varepsilon \sum_{i=1}^l (\beta_i + \beta_i^*) + \sum_{i=1}^l y_i (\beta_i + \beta_i^*) \\ \text{s. t. } \sum_{i=1}^l (\beta_i - \beta_i^*) = 0 \\ (0 \leq \beta_i; \beta_i^* \leq C; i = 1, 2, \dots, l) \end{cases} \quad (10)$$

Where β, β^* were Lagrange multiplier, Q was kernel function ($K(x_i, x_j) = \boldsymbol{\varphi}(x_i)^T \boldsymbol{\varphi}(x_j)$).

The approximation function was a decision function

$$f(x) = \sum_{i=1}^l (-\beta_i + \beta_i^*) K(x_i, x) + b \quad (11)$$

SVR kernel function $K(x_i, x_j)$ determined structure and characteristics of high dimensional space, and then determined the performance of the algorithm. RBF kernel function was used to fit regression model. ε and C was important parameters for computation time and accuracy of the model. ε was set to 10, C was set to

0.2.

2.3.3 Converse modeling

Theoretical front wheel turning angle α_m was calculated by real-time location information and running speed. Meanwhile the relationship between α_m and α_r was identified by inverse model based on SVR. modeling specific steps:

(1) The data set $A: \{\alpha_r, \alpha_m\}$ was acquired by 80 seconds for model has good timeliness. The frequency of collecting data set was 2 Hz in view of localization frequency. The new data would replace the old data before 80 s, and set A contains 160 data.

(2) The granularity data set A was obtained by the dynamic Gauss-granularity.

(3) Regression model $f(\alpha_r)$ of set $\{(\alpha_{ri}, \alpha'_{mi}), i = 1, 2, \dots, n', n' = 24\}$ was identified by support vector regression.

The inverse-model was used to correct output value of the pure pursuit model. Revised front wheel turning angle α' was calculated by inverse function $f^{-1}(\alpha_p)$ of inverse-model.

2.3.4 Simulation of GSVR inverse-model

In order to test the performance of model, the inverse-model was emulated. Test was used the navigation system of Dongfanghong LX - 854 type tractor. The collection frequency θ was 2 Hz and front wheel turning angle α_r was 10 Hz. According to experimental data, the model of tractor course was simulated by using the inverse-model and the kinematic model. Both results were compared. The simulation steps were as follow:

(1) Inverse-model was established by SVR modeling method when the tractor navigation system was linear tracking.

(2) Simulation rate of heading angle θ'_{kin} was calculated by kinematics model and turning angle α_r . Simulation heading angle θ_{kin} was integral of θ'_{kin} .

(3) α_m was revised α_r by inverse-model. Inverse-model rate of heading angle θ'_{GSVR} was calculated by kinematics model and α_m . Inverse-model heading angle θ_{GSVR} was integral of θ'_{GSVR} .

The initial heading angle of simulation experiment was -0.21° , and simulation forecast time was 30 s. The results of model comparison were shown in Fig. 6a. α_r equaled α_m in the ideal modle which does not consider influence of tire longitudinal slip, the sensor

system error and pavement properties. $f(\alpha_r)$ was different with ideal model, and the difference was corrected ideal model by $f(\alpha_r)$. The comparison results of inverse-model simulation and actual of heading course were shown in Fig. 6b. The average prediction difference between simulation of kinematics model and actual heading course was 1.43° . The average prediction difference between simulation of inverse-model and actual heading course was 0.26° . The simulation experiments showed that the inverse-model has better forecasting ability and higher accuracy.

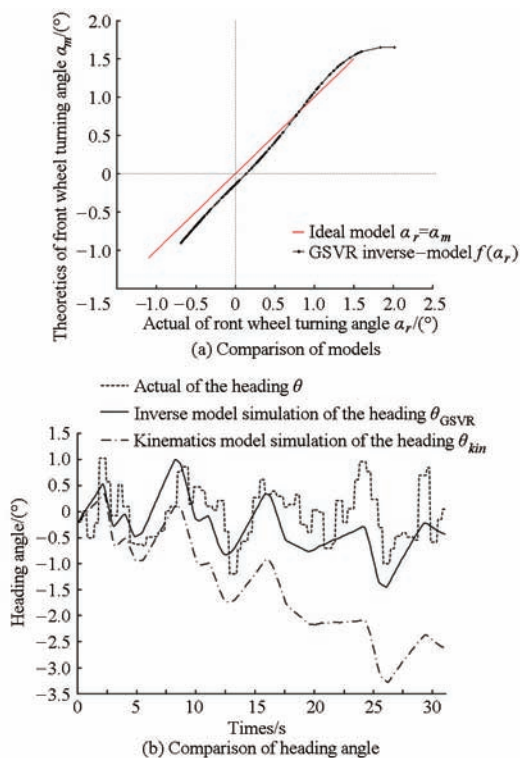


Fig. 6 Contrast diagram of simulation experiment

3 Experimentation of navigation controller

The controller of navigation based on SVR inverse-model used MFC (Microsoft foundation classes) framework with C++ program. It was loaded into the TPC 6000 - 6100T type industrial control computer. The controller experiment was carried out on LX - 854 tractor navigation system for direct-seeding combined planter (Fig. 7). Using Sinan M300 RTK - GNSS system to obtain the tractor navigation and position information, acquisition frequency of position information was 2 Hz, and horizontal positioning accuracy was $\pm (10 + 1 \times 10^{-6} D)$ mm. The performance experiment, comparison experiment and



Fig. 7 Navigation system of agricultural machine

1. System of terminal
2. Electronic steering operator
3. Angular transducers
4. RTK - GNSS

field experiment for navigation system were conducted, respectively.

3.1 Performance experiment of navigation system

The performance experiment of navigation controller was conducted on standard cement road in Huazhong Agricultural University, and the tracking controller used SVR inverse model. The equation of target line was calculated by position of two ends. The penalty coefficient C and epsilon insensitive loss factor ε of support vector regression (SVR) were 10 and 0.2. SVR used the Gauss kernel function, and the parameters of pure pursuit model were set up by Eq. (5). The speed v of tractor was 1.2 m/s, and the experiment was carried out in 3 groups. Lateral deviation of line tracking of navigation system was recorded. The sampling rate was 2 Hz. The experiment results were showed in Tab. 1, and the lateral deviation of No. 1 experiment was showed in Fig. 1. The results showed that the controller had smaller characteristics of maximum lateral deviation and higher tracking accuracy.

Tab. 1 Performance experimental results of straight line path

| Experiment No. | Maximum lateral deviation/m | Mean absolute deviation/m | Standard deviation/m | Driving distance/m |
|----------------|-----------------------------|---------------------------|----------------------|--------------------|
| 1 | 0.061 4 | 0.015 4 | 0.016 9 | 168 |
| 2 | 0.055 8 | 0.014 5 | 0.017 8 | 140 |
| 3 | 0.057 3 | 0.014 9 | 0.017 3 | 125 |
| Mean | 0.058 2 | 0.014 9 | 0.017 3 | 144 |

3.2 Comparison experiment of navigation system

Comparison experiment of navigation controller was conducted on standard cement road. Conventional

tracking controllers used pure pursuit model with unrevised front wheel angle α . According to different driving speed, the level of experiment speed was divided into five levels: 0.6 m/s, 0.8 m/s, 1.0 m/s, 1.2 m/s and 1.4 m/s. The results of experiment were showed in Tab. 2, which showed that the maximum lateral deviation of inverse model group were reduced 0.014 6 m, 0.022 0 m, 0.038 3 m, 0.036 8 m and 0.058 3 m, respectively, and the average absolute deviation decreased 0.006 0 m, 0.009 4 m, 0.011 2 m, 0.016 6 m and 0.027 9 m, respectively. The

Tab. 2 Comparative experimental results of straight line path

| Level | Average speed/ ($\text{m}\cdot\text{s}^{-1}$) | Control method | Maximum lateral deviation/m | Mean absolute deviation/m | Standard deviation/m | Driving distance/m |
|-------|--|----------------|--------------------------------|------------------------------|-------------------------|-----------------------|
| 1 | 0.698 | Inverse model | 0.030 0 | 0.007 2 | 0.008 8 | 112 |
| | 0.624 | Comparison | 0.044 6 | 0.013 2 | 0.015 7 | 125 |
| 2 | 0.786 | Inverse model | 0.039 3 | 0.014 5 | 0.014 8 | 112 |
| | 0.800 | Comparison | 0.061 3 | 0.023 9 | 0.014 8 | 144 |
| 3 | 1.026 | Inverse model | 0.040 4 | 0.012 8 | 0.015 8 | 134 |
| | 0.963 | Comparison | 0.078 7 | 0.024 0 | 0.017 1 | 144 |
| 4 | 1.218 | Inverse model | 0.057 3 | 0.014 9 | 0.017 3 | 125 |
| | 1.203 | Comparison | 0.094 1 | 0.031 5 | 0.020 3 | 102 |
| 5 | 1.485 | Inverse model | 0.062 0 | 0.019 2 | 0.019 4 | 99 |
| | 1.361 | Comparison | 0.120 3 | 0.047 1 | 0.043 4 | 70 |

3.3 Field experiment of navigation system

Navigation system test was conducted in rape field base of Huazhong Agricultural University in 21 May 2015. The plots length was 50 m. Experiment used Dongfanghong LX-854 tractor hanging 2BFQ-6 type direct-seeding combined dual purpose planter for rapeseed. In the experiment, the tracking controller based on SVR model and the conventional models were used respectively for straight line tracking. The driving speed was 0.5 m/s, and results of experiment were showed in Tab. 3, which showed that pure pursuit control method based on SVR inverse-model was suitable operation for planter in field, and control precision was lower compared with road test. Because the turning characteristics are influenced by front positive pressure, land leveling, the whole of the machine rigidity, soil solid degree, soil moisture and vegetation cover and other factors when planter worked in the field, it was more difficult to deduce tractor driving model of field from dynamic point. So it was more feasible and effective to establish a inverse model for improving path tracking accuracy in the field navigation.

results showed that the controller based on SVR inverse model has better control precision and speed adaptability.

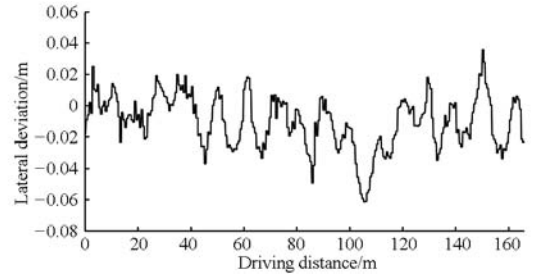


Fig. 8 Lateral deviation diagram of No. 1 straight line path

Tab. 3 Experiment results of field straight line path

| Control method | Maximum lateral deviation/m | Mean absolute deviation/m | Standard deviation/m |
|-------------------|-----------------------------------|---------------------------------|-------------------------|
| Inverse model | 0.088 7 | 0.036 1 | 0.043 3 |
| Comparison | 0.127 9 | 0.055 3 | 0.037 6 |

4 Conclusions

(1) Navigation system of Dongfanghong LX-854 tractor was constructed and pure tracking control method based on SVR inverse model was studied. In order to achieve tracking control optimization method, SVR inverse-model was used to correct control error that caused by simplification kinematics model. The results of control method for road linear tracking experiment showed that the driving distance was longer than 125 m, speed v was 1.2 m/s, the maximum horizontal deviation was less than 0.061 4 m and the absolute average deviation was not more than 0.015 4 m. The method had higher precision and speed adaptability compared with conventional tracking control method. The results of field experiment showed that pure pursuit control method based on SVR inverse-

model was suitable for planter in field.

(2) The accuracy of field experiment was lower than that of pavement experiment because the precision was influenced by friction coefficient of tire and soil, soil hardness, soil roughness, soil water content. Analyzing and studying effect of various factors on the field navigation optimized controller parameters and mathematical model would improve adaptability and precision of field navigation.

References

- [1] Hu Jingtao, Gao Lei, Bai Xiaoping, et al. Review of research on automatic guidance of agricultural vehicles [J]. Transactions of the CSAE, 2015, 31(10): 1 – 10. (in Chinese)
- [2] Ji Changying, Zhou Jun. Current situation of navigation technologies for agricultural machinery [J]. Transactions of the Chinese Society for Agricultural Machinery, 2014, 45(9): 44 – 54. (in Chinese)
- [3] Luo Xiwen, Zhang Zhigang, Zhao Zuoxi, et al. Design of DGPS navigation control system for Dongfanghong X – 804 tractor [J]. Transactions of the CSAE, 2009, 25(11): 139 – 145. (in Chinese)
- [4] Fuhong Dong, Wolfgang Heinemann, Roland Kasper. Development of a row guidance system for an autonomous robot for white asparagus harvesting [J]. Computers and Electronics in Agriculture, 2011, 79(2): 216 – 225.
- [5] Saifia D, Chadli M, Karimi H R. Fuzzy control for electric power steering system with assist motor current input constraints [J]. Journal of the Franklin Institute, 2014, 31: 1 – 14.
- [6] Ding Youchun, Wang Shumao. Vision navigation control system for combine harvester [J]. Transactions of the Chinese Society for Agricultural Machinery, 2010, 41(5): 137 – 143. (in Chinese)
- [7] Han Keli, Zhu Zhongxian, Mao Enrong, et al. Joint control method of speed and heading of navigation tractor based optimal control [J]. Transactions of the Chinese Society for Agricultural Machinery, 2013, 44(2): 165 – 170. (in Chinese)
- [8] Lü Antao, Song Zhenghe, Mao Enrong. Optimized control method for tractor automatic steering [J]. Transactions of the CSAE, 2006, 22(8): 116 – 119.
- [9] Li Taochang, Hu Jingtao, Gao Lei, et al. Agricultural machine path tracking method based on fuzzy adaptive pure pursuit model [J]. Transactions of the Chinese Society for Agricultural Machinery, 2013, 44(1): 205 – 210. (in Chinese)
- [10] Huang Peichen, Luo Xiwen, Zhang Zhigang. Control method of headland turning based on improved pure pursuit mode for agricultural machine [J]. Computer Engineering and Applications, 2010, 46(21): 216 – 219. (in Chinese)
- [11] Zou Yanyan, Wu Yuxuan, Song Zhenyu, et al. Design of fuzzy controllers based on improved genetic algorithms [J]. Control Theory and Applications, 2013, 32(11): 6 – 10. (in Chinese)
- [12] Meng Qingkuan, Qiu Ruicheng, Zhang Man, et al. Navigation system of agricultural vehicle based on fuzzy logic controller with the improved particle swarm optimization algorithm [J]. Transactions of the Chinese Society for Agricultural Machinery, 2015, 46(3): 29 – 36. (in Chinese)
- [13] Erkan Kayacan, Erdal Kayacan, Herman Ramon, et al. Towards agrobots: identification of the yaw dynamics and trajectory tracking of an autonomous tractor [J]. Computers and Electronics in Agriculture, 2015, 115: 78 – 87.
- [14] Bai Xiaoping, Hu Jingtao, Gao Lei, et al. Navigation system of agricultural vehicle based on fuzzy logic controller with the improved particle swarm optimization algorithm [J]. Transactions of the Chinese Society for Agricultural Machinery, 2015, 46(2): 1 – 7. (in Chinese)
- [15] Zhu Maofei, Chen Wuwei, Xia Guam. Vehicle chassis decoupling control based on neural network inverse method [J]. Transactions of the Chinese Society for Agricultural Machinery, 2011, 42(12): 13 – 17. (in Chinese)
- [16] Hamzaoui Y El, Rodríguez J A, Hernandez J A, et al. Optimization of operating conditions for steam turbine using an artificial neural network inverse [J]. Applied Thermal Engineering, 2015, 75: 648 – 657.
- [17] Guo Hangang. Research on model selection for support vector regression and application of it [D]. Changsha: National University of Defense Technology, 2006.
- [18] Zhang Wenyu, Ding Youchun, Liao Qingxi, et al. Variable universe fuzzy controller for tractor hydraulic steering [J]. Transactions of the Chinese Society for Agricultural Machinery, 2015, 46(3): 43 – 50. (in Chinese)
- [19] Bao Ruixin, Jia Min, Edoardo Sabbioni, et al. Vehicle state and parameter estimation under driving situation based on extended Kalman particle filter method [J]. Transactions of the Chinese Society for Agricultural Machinery, 2015, 46(2): 301 – 306. (in Chinese)

基于 SVR 逆向模型的拖拉机导航纯追踪控制方法

张闻宇 丁幼春 王雪玲 张 幸 蔡 翔 廖庆喜

(华中农业大学工学院, 武汉 430070)

摘要: 针对行驶过程中轮胎侧滑量、路面性质等不确定性因素导致传统拖拉机二轮运动学模型难以准确描述拖拉机运动轨迹的问题,提出了一种基于 SVR(Support vector regression)逆向模型的拖拉机导航纯追踪控制方法。采用粒度支持向量回归(Granular support vector regression,GSVR)方法建立了拖拉机前进航向的逆向模型,实时获得实际转弯曲率与运动学理论转弯曲率的函数关系,逆向模型对纯追踪导航模型输出进行校正提高了纯追踪导航控制方法的适应性和动态性能。拖拉机导航系统的路径追踪路面试验结果表明:当行驶距离大于 125 m、行驶速度为 1.2 m/s 时,直线追踪最大横向偏差小于 0.061 4 m,较常规纯追踪模型导航方法具有更好的直线追踪性能;田间试验结果表明:该导航控制方法适用于 2BFQ-6 型油菜精量联合直播机自动对行作业。

关键词: 拖拉机; 导航; 逆向模型; 支持向量回归; 纯追踪模型

中图分类号: S225.3 **文献标识码:** A **文章编号:** 1000-1298(2016)01-0029-08

Pure Pursuit Control Method Based on SVR Inverse-model for Tractor Navigation

Zhang Wenyu Ding Youchun Wang Xueling Zhang Xing Cai Xiang Liao Qingxi

(College of Engineering, Huazhong Agricultural University, Wuhan 430070, China)

Abstract: Considering the fact that uncertain tire sliding and uncertain pavement lead to trajectory of tractor could not be accurately described by kinematic model, a pure pursuit control method based on SVR inverse-model was proposed for agricultural machine navigation. This paper analyzed and determined the main structure and technical parameters of the method. The inverse-model of forward heading in tractor was established by using the method of granular support vector regression, and the corresponding relation function of kinematic theoretical curvature and actual curvature was obtained. The error of the output of the pure pursuit navigation model was corrected by inverse-model, thus the adaptability and dynamic performance of pure pursuit control method were improved. The path tracking experiments carried out on navigation system of the tractor and the pavement experiment results showed that the maximum of linear tracing pitch yaw roll error was less than 0.061 4 m, when the speed of agricultural machinery was 1.2 m/s and path length was longer than 125 m. Compared with the method of conventional pure pursuit navigation model, the pure pursuit control method based on SVR inverse-model has better linear racing performance. Field experiment results concluded that the maximum lateral deviation was 0.088 7 m, when the running speed of the tractor was 0.5 m/s, and the proposed controller significantly improved precision of field experiment. Based on the path tracking experiments and field experiments results, the navigation control method could be applied to automatic row-controlled operation of 2BFQ-6 type direct-seeding combined dual purpose planter for rapeseed.

Key words: tractor; navigation; inverse-model; support vector regression; pure pursuit model

收稿日期: 2015-07-09 修回日期: 2015-08-09

基金项目: 国家油菜产业技术体系专项(CARS-13)、国家公益性行业(农业)科研专项经费项目(201503116-6)、中央高校基本科研业务费项目(2013PY033、2014PY033)和武汉市高新技术产业科技创新团队项目(2014070504020240)

作者简介: 张闻宇(1985—),男,博士生,主要从事自动控制、油菜直播机导航研究,E-mail: zhangwy@webmail.hzau.edu.cn

通信作者: 廖庆喜(1968—),男,教授,博士生导师,主要从事油菜机械化生产技术与装备研究,E-mail: liaoqx@mail.hzau.edu.cn

引言

农机路径跟踪控制方法是农机智能导航核心技术^[1-2]。国内外有众多学者对路径跟踪控制方法进行了研究,其中主要包括PID(Proportion integration differentiation)控制^[3-4]、模糊控制^[5-6]、最优控制^[7-8]和纯追踪控制^[9-10]等方法,PID控制和模糊控制属于不依靠具体数学模型的控制方法,最优控制和纯追踪控制则依赖于具体数学模型。李逃昌等^[9]、邹彦艳等^[11]和孟庆宽等^[12]分别使用模糊控制、遗传算法和粒子群算法对控制器参数进行优化,而针对数学模型进行优化的较少。Erkan Kayacan等^[13]使用激励响应法辨识了逆向运动学模型,该线性模型优化了运动学模型,但线性模型的拟合度有限;白晓平等^[14]使用自校正控制器对运动学模型进行校正,其修正方法改善了曲线路径的跟踪效果,但其校正精度对直线跟踪效果改善不显著,要从建模角度改善直线跟踪效果,则需要建立精度更高更符合实际过程的数学模型;朱茂飞等^[15]、Hamzaoui等^[16]使用神经网络的方法逆向辨识系统模型,神经网络方法具有较高的鲁棒性和非线性拟合能力,但训练需要大量样本,实时运算性能较弱且容易陷入局部极小解。

为了建立高精度拖拉机导航模型,从而提高拖拉机直线跟踪精度,提出一种基于SVR(Support vector regression)逆向模型的拖拉机导航纯追踪控制方法。SVR方法是将支持向量机(Support vector machine, SVM)方法扩展到回归拟合领域中的一种高效回归方法。依据结构风险最小化归纳原则(Structural risk minimization, SRM),采用小样本和统计学习方法建立回归模型,较常规方法更稳定,泛化能力更强^[17]。本文依据该控制方法设计路径跟踪控制器,于油菜精量联合直播机的配套动力东方红-LX854型拖拉机导航系统上进行试验。

1 拖拉机导航系统结构

导航系统以油菜精量联合直播机配套动力东方红-LX854型拖拉机为研究对象。该系统由硬件和软件组成。硬件部分由RTK-GNSS系统、DWQT-BZ-V-60-G型角度传感器、NI-USB-6216型多功能数据卡、TPC6000-6100T型工控机和转向执行机构组成;软件部分为基于SVR逆向模型纯追踪控制器。使用司南M300 RTK-GNSS系统获取位姿信息,采用DWQT-BZ-V-60-G型角度传感器和NI-USB-6216型多功能数据卡采集前轮转角信

号,导航控制器对位姿信息和转角信号进行处理并运算输出转向控制信号,全液压阀转向控制系统依据控制信号作出相应的执行动作实现拖拉机导航作业。拖拉机导航系统结构如图1所示。

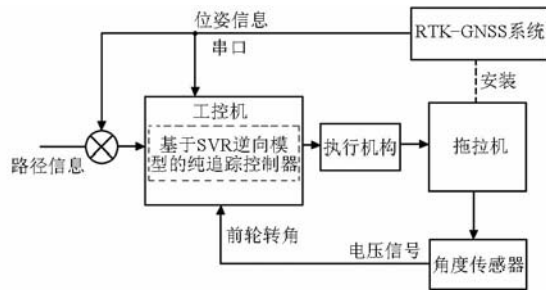


图1 拖拉机导航系统结构示意图

Fig.1 Structure diagram of navigation system

2 基于SVR逆向模型的纯追踪控制器设计

基于SVR逆向模型的纯追踪控制器由卡尔曼滤波器(Kalman filter)、纯追踪模型、粒度支持向量(Granular support vector regression, GSVR)逆向模型和转向变论域模糊控制器^[18]4部分构成。该控制器结构如图2所示。图中, d 为经过卡尔曼滤波的横向偏差(拖拉机定位位置与预定路径的垂直距离); θ 为经过卡尔曼滤波的航偏角(拖拉机前进航角与路径方向角的偏差); α_p 为纯追踪模型的前轮转角期望值; α' 为通过GSVR逆向模型校正后的前轮转角期望值; α_r 为拖拉机前轮实时转角。

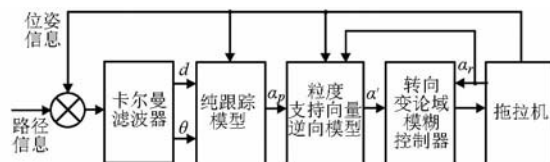


图2 基于SVR逆向模型的纯追踪控制器结构框图

Fig.2 Schematic block of pure pursuit control method based on SVR inverse-model

2.1 卡尔曼滤波器设计

使用的RTK-GNSS定位系统为司南M300系统。定位误差会影响控制器导航品质,该误差受定位系统精度、拖拉机倾角、路况和采样间隔等因素影响。为减小定位系统误差引入了卡尔曼滤波^[19]。运用卡尔曼插值滤波器分别对RTK-GNSS定位系统采集的横向偏差和航向偏差信息进行滤波处理。依据前期试验数据分析,其中横向偏差 d 的过程激励噪声协方差 Q_d 设为0.1,观测噪声协方差 R_d 设为0.1;航偏角 θ 的过程激励噪声协方差 Q_θ 设为0.6,观测噪声协方差 R_θ 设为0.8。并对定位采样间隔进行频率为10 Hz的卡尔曼插值预测,以提高导航速度适应性。

2.2 纯追踪导航控制器设计

2.2.1 拖拉机运动学模型简化

本文的控制对象为东方红-LX854型拖拉机。由于轮胎侧滑、车轴刚度等因素影响四轮车体模型的建立,且大部分因素难以准确测量。故采用简化二轮车运动学模型^[15]。由简化二轮车运动学模型可以推导出

$$\theta' = \frac{v \tan \alpha}{l} = \gamma v \quad (1)$$

式中 θ' ——拖拉机航偏角变化率

α ——拖拉机转角期望值

v ——拖拉机前进速度

l ——拖拉机轴距

γ ——拖拉机转弯曲率

2.2.2 纯追踪几何模型构建与改进

纯追踪模型是依据拖拉机的运动学方程和几何学方程描述拖拉机在固定前视距下前进路径的模型^[10]。纯追踪模型几何学示意图如图3所示。图中, L_d 为前视距, R 为转弯半径, O 为转弯圆心。

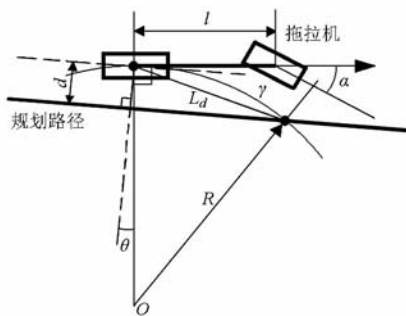


图3 纯追踪几何模型示意图

Fig.3 Geometric diagram of pure pursuit model

依据如图2所示的纯追踪模型的几何学关系,可得

$$\gamma = \frac{2(d \cos \theta - \sqrt{L_d^2 - d^2} \sin \theta)}{L_d^2} \quad (2)$$

综合式(1)和式(2)可计算获得前轮转角的期望值 α 为

$$\alpha = \arctan \frac{2l(d \cos \theta - \sqrt{L_d^2 - d^2} \sin \theta)}{L_d^2} \quad (3)$$

通过式(3)可知在前视距 L_d 预设的情况下前轮转角期望值 α 直接由横向偏差 d 和航偏角 θ 决定。面对不同行驶速度下轮胎摩擦因数和侧滑量的差异,而可控参数仅为 L_d ,无法灵活调整控制策略。所以本文在该模型中引入了2个调节系数 ξ_1 和 ξ_2 ,改进模型中的系数 ξ_1 影响 d 的控制效力,系数 ξ_2 影响 θ 的控制效力。系数 ξ_1 和 ξ_2 分别影响了追踪系统的控制精度和稳定性,即

$$\alpha = \arctan \frac{2l(\xi_1 d \cos \theta - \xi_2 \sqrt{L_d^2 - d^2} \sin \theta)}{L_d^2} \quad (4)$$

前视距 L_d 、系数 ξ_1 和系数 ξ_2 随拖拉机行驶速度 v 的变化而变化。随着拖拉机速度 v 的提高,控制系统稳定性更为重要。高速行驶时减少 ξ_1 、增加 ξ_2 和 L_d ,在保证精度的情况下提高系统稳定性,对应关系为

$$L_d = \begin{cases} 1.6 + \min(1.5(v - 0.7), 1.6) & (v > 0.7) \\ 1.6 & (v \leq 0.7) \end{cases} \quad (5)$$

$$\xi_1 = \begin{cases} 1 & (v > 0.7) \\ 1 + 0.6(0.7 - v) & (v \leq 0.7) \end{cases}$$

$$\xi_2 = \begin{cases} 1 + \min(0.5(v - 0.7), 1.2) & (v > 0.7) \\ 1 & (v \leq 0.7) \end{cases}$$

本文的纯追踪模型控制器是根据式(4)和式(5)设计完成。

2.3 粒度支持向量逆向模型构建

由于轮胎侧滑、路面性质、车辆倾角和传感器系统误差等因素影响,简化的二轮车运动学模型无法准确描述拖拉机的运动轨迹。由于轮胎与地面之间的作用关系难以用线性方程描述,拖拉机的各项状态参数不易准确测量,从动力学模型的角度正向推导建立精确的数学模型会遇到较大的困难。故本文从建立逆向模型的角度提高运动学模型的精度。采集实时记录的前轮转角 α_r 和拖拉机实际航偏角变化率 θ' 数据,通过SVR方法逆向建立理论前轮转角和实际前轮转角关系模型,该逆向模型可以用于修正简化的运动学模型引起的控制误差。同时由于 θ' 数据误差较大无法直接建模,本文对原始数据进行了动态高斯粒度预处理。所设计的粒度支持向量(GSVR)逆向模型结构如图4。图中, $\{\alpha_r, \alpha_m\}$ 为高斯粒度数据集。

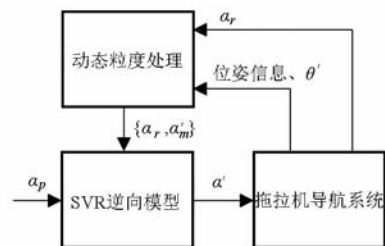


图4 粒度支持向量逆向模型结构图

Fig.4 Structure of inverse-model by granular support vector regression

2.3.1 动态高斯粒度处理

为建立实际转弯曲率 γ_r 与理论转弯曲率 γ_m 的对应关系,引入理论前轮转角 α_m 。导航系统通过记录数据获得实际转弯曲率 γ_r 和实际前轮转角 α_r ,分

别依据式(1)推导出对应的理论前轮转角 α_m 和理论转弯曲率 γ_m 为

$$\begin{cases} \alpha_m = \arctan(\gamma_r l) = \arctan\left(\frac{\theta'}{v} l\right) \\ \gamma_m = \frac{\tan \alpha_r}{l} \end{cases} \quad (6)$$

由式(6)可知,实际转弯曲率与理论转弯曲率对应关系问题可转换为理论前轮转角 α_m 和实际前轮转角 α_r 的对应关系问题: $\alpha_m = f(\alpha_r)$ 。当纯追踪模型计算出前轮转角期望值 α_p 后,代入该对应关系模型即可获得修正后的前轮转角期望值 α' 。 α_p 对应的是纯追踪导航模型计算的理想转弯曲率,而 α' 则是达到该理想转弯曲率实际所需要的前轮转角期望值。

将拖拉机航向变化率 θ' 和行驶速度 v 代入式(6)计算获得 α_m ,拖拉机实际航偏角变化率 θ' 数据由定位数据计算获得。RTK-GNSS系统的定位信号频率为2 Hz,所以 α_m 数据获取频率为2 Hz。前轮转角由控制终端内的NI-USB-6216型板卡采集,采集频率为5 000 Hz,每500个数据求平均得转角数据,获取采集频率为10 Hz。为使 α_r 、 α_m 具有相同的获取频率,本文对定位信号采集间隔内的转角数据求取平均值,将该值与 α_m 组合成为待辨识的数据集 $A: \{\alpha_r, \alpha_m\}$ 。

测量系统误差导致拖拉机航偏角变化率 θ' 数据误差较大,一段时间实际采集的 α_r 和计算获得的 α_m 数据对应集分布图如图5。由于数据庞杂,直接对数据集 A 进行SVR拟合建模效率和精确度都很低,无法获得所需的对应关系,同时也很难以此提高直线追踪精度。

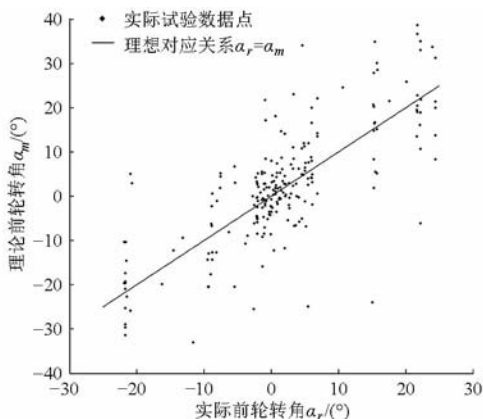


图5 理论与实际前轮转角关系图

Fig. 5 Relation graph of theory and practice front wheel angle

针对上述精确模型难以获得的问题,本文采用了纵向高斯粒度的方法对数据进行预处理,将一定范围内的数据按一定的规则替换为一个粒度。由于

前轮转角 α_r 的测量环节少且测量误差小,可认为 α_r 是准确值。所以采用纵向粒化处理数据,步骤为:

(1)以 α_{ri} 为粒划中心,将信息粒宽度 2μ 内的所有 (α_r, α_m) 数据构建成一个粒度。信息粒的粒划范围设为 $[\alpha_{ri} - \mu, \alpha_{ri} + \mu]$ 。

(2)对范围内的 α_m 数据以 α_{ri} 为中心点进行高斯加权平均

$$\begin{cases} w_j = e^{-|\alpha_r - \alpha_{ri}| / (2\sigma^2)} \\ \alpha'_{mi} = \frac{\sum_{j=1}^n w_j \alpha_{mj}}{\sum_{j=1}^n w_j} \end{cases} \quad (7)$$

式中 j ——信息粒范围内的数据序列号

n ——信息粒范围内的样本量

w_j ——高斯权值

σ ——高斯函数标准差

α'_{mi} ——信息粒的粒度

(3)计算出信息粒的粒度 α'_{mi} ,信息粒内的数据集粒划为粒度 $(\alpha_{ri}, \alpha'_{mi})$ 。

数据集 A 的整体宽度由前轮转角 α_r 数据范围决定。拖拉机处于转弯或跟踪的调整状态时 α_r 的浮动较大,范围能达到 $\pm 10^\circ$,拖拉机稳态跟踪时 α_r 的浮动很小,范围在 $\pm 2^\circ$ 。使用固定宽度 2μ 粒划方法适应性很差,不能获得良好的信息处理效果,降低了模型的泛化能力,所以本文采用动态粒度的方法解决粒度适应性问题,使信息粒的宽度 2μ 随数据集 A 的整体宽度变化而变化。数据集的动态粒度计算步骤如下:

(1)根据原始数据集 A 的宽度范围 $\alpha_r \in [\min(\alpha_r), \max(\alpha_r)]$ 计算划分信息粒的宽度 2μ , $\mu = (\max(\alpha_r) - \min(\alpha_r)) / n'$,其中 $n' = 24$, n' 为划分个数。

(2)依据宽度 μ 确定信息粒的粒划中心 α_{ri} , $\alpha_{ri} = \min(\alpha_r) + i\mu$,其中 $i = 1, 2, \dots, n'$ 。

(3)依据粒划中心 α_{ri} 和粒划宽度 μ 构建信息粒,相邻的信息粒范围有部分重合,增强粒度数据线性度。高斯函数标准差 σ 设为 $\mu/2$,依据上文所述粒度算法计算出各个信息粒的粒度 α'_{mi} ,组成新的动态粒度数据集 $\{\alpha_r, \alpha'_m\}$ 。

2.3.2 SVR支持向量回归应用

运用SVR支持向量回归方法对动态粒度数据集 $\{\alpha_r, \alpha'_m\}$ 进行辨识建模。针对拟合数据 $\{(x_i, y_i), i = 1, 2, \dots, l\}$,其中 $x \in \mathbf{R}_n$, l 为样本量(本文数据集中 α_r 对应 x , α'_m 对应 y)。支持向量回归采用高维空间线性函数 $f(x) = \mathbf{w}^T \boldsymbol{\varphi}(x) + b$ 进行拟合, \mathbf{w} 为权值向量, $\boldsymbol{\varphi}(x)$ 为非线性映射函数, b 为偏置项。该方

法引入不敏感损失因子 ε , 建立损失函数 L

$$L(y, f(x), \varepsilon) = \begin{cases} 0 & (|y - f(x)| \leq \varepsilon) \\ |y - f(x)| - \varepsilon & (|y - f(x)| > \varepsilon) \end{cases} \quad (8)$$

定义当模型值与实际值误差小于 ε 则无损失, 以提高该方法的鲁棒性。

针对高维空间线性函数依据 SRM 原则使其风险最小化, 等价于求 $\|w\|^2$ 最小化问题, 引入松弛因子 ζ_i 和惩罚系数 C 来控制拟合函数的复杂性, 减少运算时间。上述问题转换为

$$\begin{cases} \min_{w, b, \zeta, \zeta^*} \frac{1}{2} w^T w + C \sum_{i=1}^l \zeta_i + C \sum_{i=1}^l \zeta_i^* \\ \text{s. t.} & w^T \varphi(x_i) + b - y_i \leq \varepsilon + \zeta_i \\ & y_i - w^T \varphi(x_i) - b \leq \varepsilon + \zeta_i^* \\ & (\zeta_i \geq 0, \zeta_i^* \geq 0, i = 1, 2, \dots, l) \end{cases} \quad (9)$$

为求解上述最小化问题, 引入拉格朗日函数。使问题进一步转换为对偶问题

$$\begin{cases} \min_{\beta, \beta^*} \left(\frac{1}{2} (\beta - \beta^*)^T Q (\beta - \beta^*) + \varepsilon \sum_{i=1}^l (\beta_i + \beta_i^*) + \sum_{i=1}^l y_i (\beta_i + \beta_i^*) \right) \\ \text{s. t.} & \sum_{i=1}^l (\beta_i - \beta_i^*) = 0 \\ & (0 \leq \beta_i, \beta_i^* \leq C; i = 1, 2, \dots, l) \end{cases} \quad (10)$$

式中 β, β^* ——拉格朗日乘子

Q 为核函数 $K(x_i, x_j) = \varphi(x_i)^T \varphi(x_j)$ 。

其近似函数为决策函数

$$f(x) = \sum_{i=1}^l (-\beta_i + \beta_i^*) K(x_i, x) + b \quad (11)$$

最终回归模型 $f(x)$ 为决策函数 (式 (11))。SVR 算法中核函数 $K(x_i, x_j)$ 决定了高维空间的结构和特点, 进而决定了算法的性能。本文采用较为常用的高斯核函数 (Radial basis function, RBF), RBF 核函数拟合性能良好, 适用于该回归模型。惩罚系数 C 和不敏感损失因子 ε 也是影响模型的运算时间和精度的重要参数, 依据前期试验数据的拟合情况, 将 C 设为 10, ε 设为 0.2。

2.3.3 逆向建模

通过获取一段时间内的实时位姿信息和实时行驶速度信息推导理论前轮转角 α_m 。并逆向建立 α_m 和实际前轮转角 α_r 的对应关系模型。逆向建模具体步骤为:

(1) 获取待辨识的数据集 $A: \{\alpha_r, \alpha_m\}$ 。该数据集获取频率为 2 Hz, 其依赖于定位数据采集频率。为使该模型具有良好的时效性, 采用 80 s 的时间窗

口获取数据集。新获得数据连续收入数据集 A , 80 s 之前收入的旧数据将从数据集 A 中剔除, 数据集 A 最大包含 160 组数据。

(2) 对数据集 A 进行动态高斯粒度处理, 获得高斯粒度数据集 $\{\alpha_r, \alpha'_m\}$ 。

(3) 采用 SVR 支持向量回归方法建立高斯粒度数据集 $\{(\alpha_{ri}, \alpha'_{mi}); i = 1, 2, \dots, n'\}$ (其中 $n' = 24$) 的回归模型 $\alpha'_m = f(\alpha_r)$ 。

获得上述逆向模型后, 将其用于校正纯追踪模型的输出值。纯追踪模型依据位姿信息计算出前轮转角期望值 α_p 之后, 代入逆向模型反函数 $f^{-1}(\alpha_p)$ 计算获得修正后的前轮转角期望值 α' , 以此为拖拉机前轮控制目标。

2.3.4 GSVR 逆向模型仿真

为测试粒度支持向量 (GSVR) 逆向模型的性能进行了模型仿真。试验使用东方红 LX-854 型拖拉机导航系统, 航偏角 θ 采集频率为 2 Hz, 前轮转角 α_r 和前进速度 v 数据的采集频率为 10 Hz。根据试验数据分别使用逆向模型和运动学模型对拖拉机航向进行仿真预测, 将逆向模型仿真航向、运动学模型仿真航向和实际拖拉机航向进行对比, 仿真试验步骤为:

(1) 使拖拉机导航系统处于直线跟踪状态。依据上文所述 GSVR 逆向建模方法在线建立该系统的逆向模型 $f(\alpha_r)$ 。

(2) 前轮转角 α_r 代入运动学方程式 (1) 计算获得运动学模型仿真航偏角变化率 θ'_{kin} , 对 θ'_{kin} 进行时间积分获得运动学模型仿真航偏角 θ_{kin} 。

(3) 通过逆向模型 $f(\alpha_r)$ 计算出对 α_r 修正后的理论前轮转角 α_m 。 α_m 代入运动学方程式 (1) 计算获得逆向模型仿真航偏角变化率 θ'_{GSVR} , 对其时间积分后获得逆向模型仿真航偏角 θ_{GSVR} 。

仿真试验初始航偏角为 -0.21° , 预测时间为 30 s。模型对比结果如图 6a 所示。理想模型中 α_r 与 α_m 相等, 并没有考虑轮胎侧滑量不一致、传感器系统误差和路面性质等因素影响。 $f(\alpha_r)$ 与理想模型的具体对应关系存在差异, 该差异为 $f(\alpha_r)$ 对理想模型的修正。逆向模型仿真航偏角、运动学模型仿真航偏角和实际拖拉机航偏角对比结果如图 6b 所示。无校正预测误差随预测时间累计, 未经修正的运动学模型仿真航偏角与实际航偏角的平均预测误差为 1.43° ; 使用 $f(\alpha_r)$ 对运动学模型进行校正, 逆向模型仿真航偏角更接近于实际航偏角, 与实际航偏角的平均预测误差为 0.26° 。仿真试验表明逆向模型具有更好的预测能力和更高的模型精度。

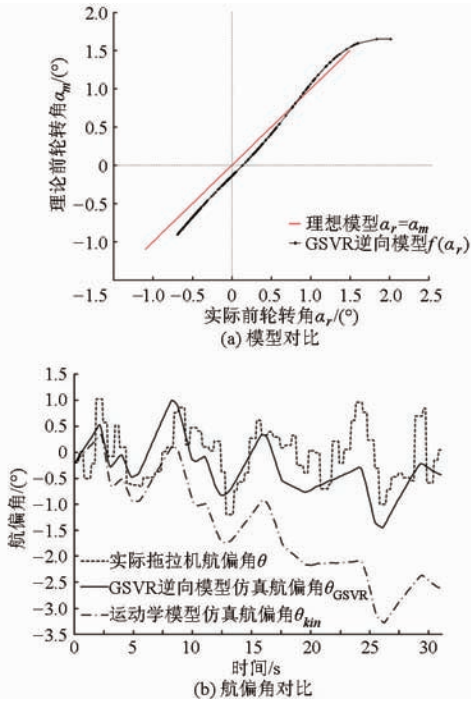


图6 仿真试验对比曲线

Fig. 6 Contrast curves of simulation experiment

3 导航控制器试验

基于SVR 逆向模型纯追踪控制器采用MFC (Microsoft foundation classes) 框架由C++程序实现, 装载于TPC 6000-6100T型工控机。控制器试验在油菜精量联合直播机配套动力东方红LX-854型拖拉机导航系统(图7)上进行。使用司南M300 RTK-GNSS型系统获取拖拉机导航的定位信息, 定位信息获取频率为2 Hz, 水平定位精度 $\pm(10 + 1 \times 10^{-6}D)$ mm, D 为RTK-GNSS移动站与基站间的距离。开展了导航控制系统性能试验、导航控制器对比试验、导航控制系统田间试验。



图7 拖拉机导航系统

Fig. 7 Navigation system of tractor

1. 导航控制终端
2. 电控转向执行机构
3. 角度传感器
4. RTK-GNSS定位系统

3.1 导航控制系统性能试验

导航控制性能试验于华中农业大学标准水泥路面进行, 使用基于SVR 逆向模型纯追踪控制器控制拖拉机跟踪目标直线, 直线方程通过两端的定位点计算获得。按SVR方法中的参数惩罚系数 C 和不敏感损失因子 ε 分别为10和0.2, 支持向量模型采用高斯核函数, 纯追踪模型参数按式(5)设置。拖拉机直线跟踪速度 $v = 1.2$ m/s, 试验进行3组。实时记录直线跟踪过程中拖拉机与期望路径的横向偏差, 采样率为2 Hz。试验结果见表1, 其中1号跟踪试验横向偏差结果如图8所示。结果表明该控制器具有最大横向偏差小、跟踪精度高的特点。

表1 直线跟踪性能试验结果

Tab. 1 Performance experimental results

| 试验序号 | of straight line path | | | m |
|------|-----------------------|----------|---------|-----|
| | 最大横向偏差 | 平均绝对横向偏差 | 标准差 | |
| 1 | 0.061 4 | 0.015 4 | 0.016 9 | 168 |
| 2 | 0.055 8 | 0.014 5 | 0.017 8 | 140 |
| 3 | 0.057 3 | 0.014 9 | 0.017 3 | 125 |
| 平均 | 0.058 2 | 0.014 9 | 0.017 3 | 144 |

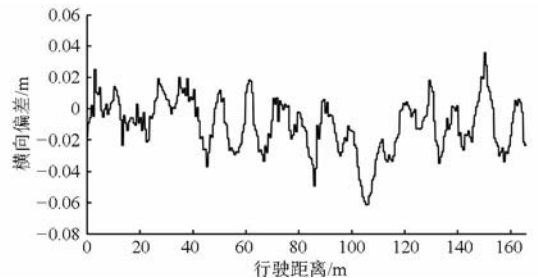


图8 1号试验直线跟踪横向偏差曲线

Fig. 8 Lateral deviation diagram of No. 1 straight line path

3.2 导航控制系统对比试验

基于SVR 逆向模型纯追踪控制器与常规纯追踪控制器的直线跟踪对比试验采用同一拖拉机导航系统, 在华中农业大学标准水泥路面展开。常规纯追踪控制器由前述纯追踪控制器构成, 不使用逆向模型对其输出的前轮转角期望值 α 进行修正。对比试验根据不同行驶速度分为5个水平, 分别为0.6、0.8、1.0、1.2、1.4 m/s, 试验结果如表2所示。5组行驶速度下, 逆向模型组相对于常规组最大横向偏差分别减少0.014 6、0.022 0、0.038 3、0.036 8、0.058 3 m, 平均绝对横向偏差分别减少0.006 0、0.009 4、0.011 2、0.016 6、0.027 9 m。结果表明基于SVR 逆向模型纯追踪控制器具有更高的控制精度和速度适应性。

表 2 拖拉机直线跟踪试验对比结果

Tab.2 Comparative experimental results of straight line path

| 水平 | 平均速度/($\text{m}\cdot\text{s}^{-1}$) | 控制方法 | 最大横向偏差/m | 平均绝对横向偏差/m | 标准差/m | 行驶距离/m |
|----|---------------------------------------|------|----------|------------|---------|--------|
| 1 | 0.698 | 逆向模型 | 0.030 0 | 0.007 2 | 0.008 8 | 112 |
| | 0.624 | 常规组 | 0.044 6 | 0.013 2 | 0.015 7 | 125 |
| 2 | 0.786 | 逆向模型 | 0.039 3 | 0.014 5 | 0.014 8 | 112 |
| | 0.800 | 常规组 | 0.061 3 | 0.023 9 | 0.014 8 | 144 |
| 3 | 1.026 | 逆向模型 | 0.040 4 | 0.012 8 | 0.015 8 | 134 |
| | 0.963 | 常规组 | 0.078 7 | 0.024 0 | 0.017 1 | 144 |
| 4 | 1.218 | 逆向模型 | 0.057 3 | 0.014 9 | 0.017 3 | 125 |
| | 1.203 | 常规组 | 0.094 1 | 0.031 5 | 0.020 3 | 102 |
| 5 | 1.485 | 逆向模型 | 0.062 0 | 0.019 2 | 0.019 4 | 99 |
| | 1.361 | 常规组 | 0.120 3 | 0.047 1 | 0.043 4 | 70 |

3.3 导航控制系统田间试验

为检验所设计控制器的田间工作性能,2015年5月21日于华中农业大学现代农业科技试验基地油菜茬田进行导航系统试验,田块长度为50m。试验采用东方红-LX854型拖拉机,后挂接2BFQ-6型油菜精量联合直播机。试验中使用基于SVR逆向模型纯追踪控制器和常规纯追踪控制器分别进行直线跟踪,行驶速度为0.5m/s,试验结果见表3。田间试验结果表明,所设计的基于SVR逆向模型纯追踪控制方法适用于控制2BFQ-6型油菜精量联合直播机进行田间对行作业,控制精度与路面试验相比较低。拖拉机挂接油菜精量直播机于田间作业时,其转弯特性会受到前轮正压力、土地平整度、机具整体刚度、土壤坚实度、土壤含水率以及植被覆盖等因素影响。由于田间影响因素比路面复杂,从动力学角度正向推导拖拉机田间行驶模型比路面行驶模型更困难,所以在田间导航作业过程中实时建立

表 3 田间直线跟踪试验结果

Tab.3 Experiment results of field straight line path

| 控制方法 | m | | |
|------|---------|----------|---------|
| | 最大横向偏差 | 平均绝对横向偏差 | 标准差 |
| 逆向模型 | 0.088 7 | 0.036 1 | 0.043 3 |
| 常规组 | 0.127 9 | 0.055 3 | 0.037 6 |

逆向模型以提高田间路径跟踪精度是更可行和有效的方法。

4 结论

(1)构建了油菜精量联合直播机配套动力东方红-LX854型拖拉机导航系统,并研究了纯追踪控制方法,在此基础上提出了基于SVR逆向模型纯追踪控制方法。采用GSVR建模方法逆向建立理论前轮转角和实际前轮转角的对应函数模型,用于修正运动学模型中转弯曲率的模型偏差,从而实现纯追踪控制方法的优化。该控制方法的路面直线跟踪试验结果表明:行驶距离大于125m,跟踪速度 v 为1.2m/s时,横向偏差最大值小于0.0614m,绝对平均偏差不大于0.0154m;与常规纯追踪控制方法相比,逆向模型方法具有更高的精度和速度适应性;田间试验表明,逆向模型方法适用于油菜精量联合直播机田间导航作业。

(2)田间试验控制精度低于路面试验,该精度受轮胎与泥土摩擦因数、土壤坚实度、土壤平整度、土壤含水率等多方面因素影响。分析研究各影响因素对田间导航的作用,并对控制器参数以及数学模型进行优化,将会提高田间路径跟踪的适应性和精度。

参 考 文 献

- 胡静涛,高雷,白晓平,等. 农业机械自动驾驶技术研究进展[J]. 农业工程学报,2015,31(10):1-10.
Hu Jingtao, Gao Lei, Bai Xiaoping, et al. Review of research on automatic guidance of agricultural vehicles[J]. Transactions of the CSAE,2015,31(10):1-10. (in Chinese)
- 姬长英,周俊. 农业机械导航技术发展分析[J]. 农业机械学报,2014,45(9):44-54.
Ji Changying, Zhou Jun. Current situation of navigation technologies for agricultural machinery[J]. Transactions of the Chinese Society for Agricultural Machinery, 2014, 45(9):44-54. (in Chinese)
- 罗锡文,张智刚,赵祚喜,等. 东方红X-804拖拉机的DGPS自动驾驶控制系统[J]. 农业工程学报,2009,25(11):139-145.
Luo Xiwen, Zhang Zhigang, Zhao Zuoxi, et al. Design of DGPS navigation control system for Dongfanghong X-804 tractor[J]. Transactions of the CSAE, 2009, 25(11):139-145. (in Chinese)
- Dong Fuhong, Wolfgang Heinemann, Roland Kasper. Development of a row guidance system for an autonomous robot for white

- asparagus harvesting[J]. *Computers and Electronics in Agriculture*, 2011, 79(2): 216 – 225.
- 5 Saifia D, Chadli M, Karimi H R, et al. Fuzzy control for electric power steering system with assist motor current input constraints [J]. *Journal of the Franklin Institute*, 2015, 352(2): 562 – 576.
- 6 丁幼春, 王书茂. 联合收获机视觉导航控制系统设计与试验[J]. *农业机械学报*, 2010, 41(5): 137 – 142.
Ding Youchun, Wang Shumao. Vision navigation control system for combine harvester[J]. *Transactions of the Chinese Society for Agricultural Machinery*, 2010, 41(5): 137 – 142. (in Chinese)
- 7 韩科立, 朱忠祥, 毛恩荣, 等. 基于最优控制的导航拖拉机速度与航向联合控制方法[J]. *农业机械学报*, 2013, 44(2): 165 – 170.
Han Keli, Zhu Zhongxiang, Mao Enrong, et al. Joint control method of speed and heading of navigation tractor based optimal control [J]. *Transactions of the Chinese Society for Agricultural Machinery*, 2013, 44(2): 165 – 170. (in Chinese)
- 8 吕安涛, 宋正河, 毛恩荣. 拖拉机自动转向最优控制方法的研究[J]. *农业工程学报*, 2006, 22(8): 116 – 119.
Lü Antao, Song Zhenghe, Mao Enrong. Optimized control method for tractor automatic steering[J]. *Transactions of the CSAE*, 2006, 22(8): 116 – 119. (in Chinese)
- 9 李逃昌, 胡静涛, 高雷, 等. 基于模糊自适应纯追踪模型的农业机械路径跟踪方法[J]. *农业机械学报*, 2013, 44(1): 205 – 210.
Li Taochang, Hu Jingtao, Gao Lei, et al. Agricultural machine path tracking method based on fuzzy adaptive pure pursuit model [J]. *Transactions of the Chinese Society for Agricultural Machinery*, 2013, 44(1): 205 – 210. (in Chinese)
- 10 黄沛琛, 罗锡文, 张智刚. 改进纯追踪模型的农业机械地头转向控制方法[J]. *计算机工程与应用*, 2010, 46(21): 216 – 219.
Huang Peichen, Luo Xiwen, Zhang Zhigang. Control method of headland turning based on improved pure pursuit mode for agricultural machine[J]. *Computer Engineering and Applications*, 2010, 46(21): 216 – 219. (in Chinese)
- 11 邹彦艳, 吴宇轩, 宋振宇, 等. 基于改进遗传算法的模糊控制器设计[J]. *自动化技术与应用*, 2013, 32(11): 6 – 10.
Zou Yanyan, Wu Yuxuan, Song Zhenyu, et al. Design of fuzzy controllers based on improved genetic algorithms[J]. *Control Theory and Applications*, 2013, 32(11): 6 – 10. (in Chinese)
- 12 孟庆宽, 仇瑞承, 张漫, 等. 基于改进粒子群优化模糊控制的农业车辆导航系统[J]. *农业机械学报*, 2015, 46(3): 29 – 36.
Meng Qingkuan, Qiu Ruicheng, Zhang Man, et al. Navigation system of agricultural vehicle based on fuzzy logic controller with the improved particle swarm optimization algorithm [J]. *Transactions of the Chinese Society for Agricultural Machinery*, 2015, 46(3): 29 – 36. (in Chinese)
- 13 Erkan Kayacan, Erdal Kayacan, Herman Ramon, et al. Towards agrobots: identification of the yaw dynamics and trajectory tracking of an autonomous tractor[J]. *Computers and Electronics in Agriculture*, 2015, 115: 78 – 87.
- 14 白晓平, 胡静涛, 高雷, 等. 农机导航自校正模型控制方法研究[J]. *农业机械学报*, 2015, 46(2): 1 – 7.
Bai Xiaoping, Hu Jingtao, Gao Lei, et al. Navigation system of agricultural vehicle based on fuzzy logic controller with the improved particle swarm optimization algorithm [J]. *Transactions of the Chinese Society for Agricultural Machinery*, 2015, 46(2): 1 – 7. (in Chinese)
- 15 朱茂飞, 陈无畏, 夏光. 基于神经网络逆系统方法的汽车底盘解耦控制 [J]. *农业机械学报*, 2011, 42(12): 13 – 17.
Zhu Maofei, Chen Wuwei, Xia Guang. Vehicle chassis decoupling control based on neural network inverse method [J]. *Transactions of the Chinese Society for Agricultural Machinery*, 2011, 42(12): 13 – 17. (in Chinese)
- 16 Hamzaoui Y El, Rodríguez J A, Hernandez J A, et al. Optimization of operating conditions for steam turbine using an artificial neural network inverse[J]. *Applied Thermal Engineering*, 2015, 75: 648 – 657.
- 17 刘靖旭. 支持向量回归的模型选择及应用研究[D]. 长沙: 国防科学技术大学, 2006.
Liu Jingxu. Research on model selection for support vector regression and application of it [D]. Changsha: National University of Defense Technology, 2006. (in Chinese)
- 18 张闻宇, 丁幼春, 廖庆喜, 等. 拖拉机液压转向变论域模糊控制器设计与试验[J]. *农业机械学报*, 2015, 46(3): 43 – 50.
Zhang Wenyu, Ding Youchun, Liao Qingxi, et al. Variable universe fuzzy controller for tractor hydraulic steering [J]. *Transactions of the Chinese Society for Agricultural Machinery*, 2015, 46(3): 43 – 50. (in Chinese)
- 19 包瑞新, 贾敏, Edoardo Sabbioni, 等. 基于扩展 Kalman 粒子滤波的汽车行驶状态和参数估计[J]. *农业机械学报*, 2015, 46(2): 301 – 306.
Bao Ruixin, Jia Min, Edoardo Sabbioni, et al. Vehicle state and parameter estimation under driving situation based on extended Kalman particle filter method [J]. *Transactions of the Chinese Society for Agricultural Machinery*, 2015, 46(2): 301 – 306. (in Chinese)